TCT: Convexifying Federated Learning using Bootstrapped Neural Tangent Kernels

Yaodong Yu
UC Berkeley
yyu@eecs.berkeley.edu

Alexander Wei
UC Berkeley
awei@berkeley.edu

Sai Praneeth Karimireddy
UC Berkeley
sp.karimireddy@berkeley.edu

Yi Ma
UC Berkeley
yima@eecs.berkeley.edu

Michael I. Jordan
UC Berkeley
jordan@cs.berkeley.edu

Abstract

State-of-the-art federated learning methods can perform far worse than their centralized counterparts when clients have dissimilar data distributions. For neural networks, even when centralized SGD easily finds a solution that is simultaneously performant for all clients, current federated optimization methods fail to converge to a comparable solution. We show that this performance disparity can largely be attributed to optimization challenges presented by *nonconvexity*. Specifically, we find that the early layers of the network do learn useful features, but the final layers fail to make use of them. That is, federated optimization applied to this non-convex problem distorts the learning of the final layers. Leveraging this observation, we propose a ***T**rain-**C**onvexify-**T**rain* (TCT) procedure to sidestep this issue: first, learn features using off-the-shelf methods (e.g., FedAvg); then, optimize a *convexified* problem obtained from the network's empirical neural tangent kernel approximation. Our technique yields accuracy improvements of up to $+36\%$ on FMNIST and $+37\%$ on CIFAR10 when clients have dissimilar data.

1 Introduction

Federated learning is a newly emerging paradigm for machine learning where multiple data holders (clients) collaborate to train a model on their combined dataset. Clients only share partially trained models and other statistics computed from their dataset, keeping their raw data local and private [53, 37]. By obviating the need for a third party to collect and store clients' data, federated learning has several advantages over the classical, centralized paradigm [14, 31, 23]: it ensures clients' consent is tied to the specific task at hand by requiring active participation of the clients in training, confers some basic level of privacy, and has the potential to make machine learning more participatory in general [43, 36]. Further, widespread legislation of data portability and privacy requirements (such as GDPR and CCPA) might even make federated learning a necessity [59].

Collaboration among clients is most attractive when clients have very different subsets of the combined dataset (*data heterogeneity*). For example, different autonomous driving companies may only be able to collect data in weather conditions specific to their location, whereas their vehicles would need to function under all conditions. In such a scenario, it would be mutually beneficial for companies in geographically diverse locations to collaborate and share data with each other. Further, in such settings, clients are physically separated and connected by ad-hoc networks with large latencies and limited bandwidth. This is especially true when clients are edge devices such as mobile phones, IoT sensors, etc. Thus, *communication efficiency* is crucial for practical federated learning. However, it is precisely under such circumstances (large data heterogeneity and low communication) that current algorithms fail dramatically [27, 48, 39, 61, 71, 1, 46, 3, 72, etc.]. This motivates our central question: *Why do current federated methods fail in the face of data heterogeneity—and how can we fix them?*

Our solution. We make two main observations: (i) We show that, even with data heterogeneity, linear models can be trained in a federated manner through gradient correction techniques such as SCAFFOLD [39]. While this observation is promising, it alone remains limited, as linear models are not rich enough to solve practical problems of interest (e.g., those that require feature learning). (ii) We shed light on why current federated algorithms struggle to train deep, nonconvex models. We observe that the failure of existing methods for neural networks is not uniform across the layers. The early layers of the network do in fact learn useful features, but the final layers fail to make use of them. Specifically, federated optimization applied to this nonconvex problem results in distorted final layers.

These observations suggest a *train-convexify-train* federated algorithm, which we call *TCT*: first, use any off-the-shelf federated algorithm [such as FedAvg, 53] to train a deep model to extract useful features; then, compute a convex approximation of the deep model using its empirical Neural Tangent Kernel (eNTK) [34, 44, 20, 51, 75], and use gradient correction methods such as SCAFFOLD to train the final model. Effectively, the second-stage features freeze the features learned in the first stage and fit a linear model over them. We show that this simple strategy is highly performant on a variety of tasks and models—we obtain accuracy gains up to 36% points on FMNIST with a CNN, 37% points on CIFAR10 with ResNet18-GN, and 16% points on CIFAR100 with ResNet18-GN. Further, its convergence remains unaffected even by extreme data heterogeneity. Finally, we show that given a pre-trained model, our method completely closes the gap between centralized and federated methods.

2 Related Work

Federated learning. There are two main motivating scenarios for federated learning (FL). The first is where internet service companies (e.g., Google, Facebook, Apple, etc.) want to train machine learning models over their users' data, but do not want to transmit raw personalized data away from user devices [60, 8]. This is the setting of *cross-device* federated learning and is characterized by an extremely large number of unreliable clients, each of whom has very little data and the collections of data are assumed to be homogeneous [37, 10, 38, 8]. The second motivating scenario is when valuable data is split across different organizations, each of whom is either protected by privacy regulation or is simply unwilling to share their raw data. Such "data islands" are common among hospital networks, financial institutions, autonomous-vehicle companies, etc. This is known as *cross-silo* federated learning and is characterized by a few highly reliable clients, who potentially have extremely diverse data. In this work, we focus on the latter scenario.

Metrics in FL. FL research considers numerous metrics, such as fairness across users [55, 47, 62], formal security and privacy guarantees [9, 60, 21, 56], robustness to corrupted agents and corrupted training data [7, 64, 19, 40, 26], preventing backdoors at test time [6, 66, 69, 52], etc. While these concerns are important, the main goal of FL (and our work) is to achieve high accuracy with minimal communication [53]. Clients are typically geographically separated yet need to communicate large deep learning models over unoptimized ad-hoc networks [37]. Finally, we focus on the setting where all users are interested in training the same model over the combined dataset. This is in contrast to model-agnostic protocols [49, 58, 3] or personalized federated learning [16, 18, 78, 13, 42, 12]. Finally, we focus on minimizing the number of rounds required. Our approach can be combined with communication compression, which reduces bits sent per round [67, 4, 24, 65].

Federated optimization. Algorithms for FL proceed in rounds. In each round, the server sends a model to the clients, who partially train this model using their local compute and data. The clients send these partially trained models back to the server who then aggregates them, finishing a round. FedAvg [53], which is the de facto standard FL algorithm, uses SGD to perform local updates on the clients and aggregates the client models by simply averaging their parameters. Unfortunately, however, FedAvg has been observed to perform poorly when faced with data heterogeneity across the clients [27, 48, 39, 61, 71, 1, 46, 3, 72, 17, etc.]. Theoretical investigations of this phenomenon [39, 76] showed that this was a result of *gradient heterogeneity* across the clients. Consider FedAvg initialized with the globally optimal model. If this model is not also optimal for each of the clients as well, the local updates will push it away from the global optimum. Thus, convergence would require a careful tuning of hyper-parameters. To overcome this issue, SCAFFOLD [39] and FedDyn [1] propose to use control variates to correct for the biases of the individual clients akin to variance

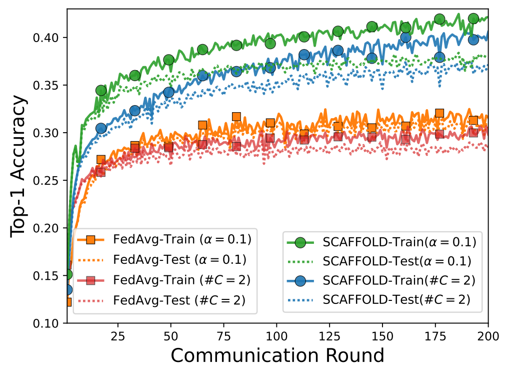

(a) Using linear model.

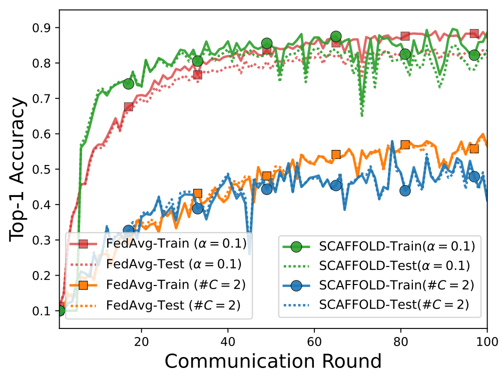

(b) Using ResNet-18.

Figure 1: Performance of FedAvg and SCAFFOLD on CIFAR10 when data are split among ten clients in two ways (`#C=2` and α=0.1). The `#C=2` split is more non-i.i.d. than the α=0.1 split. For convex problems (left), gradient correction methods such as SCAFFOLD are relatively unaffected by data heterogeneity, and consistently outperform FedAvg. However, for nonconvex problems (right), FedAvg and SCAFFOLD perform very similarly and both are strongly negatively affected by data heterogeneity.

reduction [35, 15]. This *gradient correction* is applied in every local update by the client and provably nullifies the effect of gradient heterogeneity [39, 54, 12]. However, as we show here, such methods are insufficient to overcome high data heterogeneity especially for deep learning. Other, more heuristic approaches to combat gradient heterogeneity include using a regularizer [48] and sophisticated server aggregation strategies such as momentum [28, 70, 50] or adaptivity [61, 38, 11].

A second line of work pins the blame on performance loss due to averaging nonconvex models. To overcome this, Singh and Jaggi [63], Yu et al. [81] propose to learn a mapping between the weights of the client models before averaging, Afonin and Karimireddy [3] advocates a functional perspective and replaces the averaging step with knowledge distillation, and Wang et al. [74], Li et al. [46], Tan et al. [68] attempt to align the internal representations of the client models. However, averaging is unlikely to be the only culprit since FedAvg does succeed under low heterogeneity, and averaging nonconvex models can lead to improved performance [33, 77].

Neural Tangent Kernels (NTK) and neural network linearization. NTK was first proposed to analyze the limiting behavior of infinitely wide networks [34, 44]. While NTK with MSE may be a bad approximation of real-world finite networks in general [22], it approximates the fine-tuning of a pre-trained network well [57], especially with some minor modifications [2]. That is, NTK cannot capture feature learning but does capture how a model utilizes learnt features better than last/mid layer activations.

3 The Effect of Nonconvexity

In this section, we investigate the poor performance of FedAvg [53] and SCAFFOLD [39] empirically in the setting of deep neural networks, focusing on image classification with a ResNet-18. To construct our federated learning setup, we split the CIFAR-10 dataset in a highly heterogeneous manner among ten clients. We either assign each client two classes (denoted by `#C=2`) or distribute samples according to a Dirichlet distribution with $\alpha = 0.1$ (denoted by α=0.1). For more details, see Section 5.1.

Insufficiency of gradient correction methods. Current theoretical work [e.g., 39, 61, 1, 73] attributes the slowdown from data heterogeneity to the individual clients having varying local optima. If no single model is simultaneously optimal for all clients, then the updates of different clients can compete with and distort each other, leading to slow convergence. This tension is captured by the variance of the updates across the clients [client gradient heterogeneity, see 72]. Gradient correction methods such as SCAFFOLD [39] and FedDyn [1] explicitly correct for this and are provably unaffected by gradient heterogeneity for both convex and nonconvex losses.

Table 1: Feature learning by FedAvg. We report the test accuracy of a ResNet-18 after (centralized) retraining of the last ℓ layers on CIFAR10. The earlier $(7-\ell)$ layers are frozen to either random initialization or to the weights of a FedAvg-trained model. The difference measures utility of the $(7-\ell)$ layers learnt by FedAvg. The baseline FedAvg model without additional training gets 56.9% accuracy. We see that all layers of the FedAvg model contain useful information.

Layers retrained	Accuracy (%) Random init	Accuracy (%) FedAvg init	Improvement (%) (FedAvg - Random)
1/7 last layer	35.37	77.93	42.56
2/7 last layers	67.33	87.04	19.71
3/7 last layers	80.18	89.28	9.10
4/7 last layers	88.03	90.57	2.54
5/7 last layers	91.34	91.61	0.27
6/7 last layers	91.78	91.91	0.13

These theoretical predictions are aligned with the results of Figure 1(a), where the loss landscape is convex: SCAFFOLD is relatively unaffected by the level of heterogeneity and consistently outperforms FedAvg. In particular, performance is largely dictated by the algorithm and not the data distributions. This shows that client gradient heterogeneity captures the difficulty of the problem well. On the other hand, when training a ResNet-18 model with nonconvex loss landscape, Figure 1(b) shows that both FedAvg and SCAFFOLD suffer from data heterogeneity. This is despite the theory of gradient correction applying to both convex and nonconvex losses. Further, the train and test accuracies in Figure 1(b) match quite closely, suggesting that the failure lies in optimization (not fitting the training data) rather than generalization. Thus, while the current theory makes no qualitative distinctions between convex and nonconvex convergence, the practical behavior of algorithms in these settings is very different. Such differences between theoretical predictions and practical reality suggests that black-box notions such as gradient heterogeneity are insufficient for capturing the difficulty of training deep models.

Ease of feature learning. We now dive into how a ResNet-18 trained with FedAvg (56.9% accuracy) differs from the centralized baseline (91.9% accuracy). We first apply linear probing to the FedAvg model (i.e., retraining with all but the output layer frozen). Note that this is equivalent to (convex) logistic regression over the last-layer activations. This simple procedure produces a striking jump from 56.9% to 77.9% accuracy. Thus, of the 35% gap in accuracy between the FedAvg and centralized models, 21% may be attributed to a failure to optimize the linear output layer. We next extend this experiment towards probing the information content of other layers.

Given a FedAvg-trained model, we can use centralized training to retrain only the last ℓ layers while keeping the rest of the $(7-\ell)$ layers (or ResNet blocks) frozen. We can also perform this procedure starting from a randomly initialized model. The performance difference between these two models can be attributed to the information content of the frozen $(7-\ell)$ layers of the FedAvg model. Table 1 summarizes the results of this experiment. The large difference in accuracy (up to 42.6%) indicates the initial layers of the FedAvg model have learned useful features. There continues to be a gap between the FedAvg features and random features in the earlier layers as well,[1] meaning that all layers of the FedAvg model learn useful features. We conjecture this is because from the perspective of earlier layers which perform simple edge detection, the tasks are independent of labels and the clients are i.i.d. However, the higher layers are more specialized and the effect of the heterogeneity is stronger.

4 Method

Based on the observations in Section 3, we propose *train-convexify-train* (TCT) as a method for overcoming data heterogeneity when training deep models in a federated setting. Our high-level

[1]The significant decrease in the gap as we go down the layers may be because of the skip connections in the lower ResNet blocks which allow the random frozen layers to be sidestepped. This underestimates the true utility and information content in the earlier FedAvg layers.

intuition is that we want to leverage both the features learned from applying FedAvg to neural networks and the effectiveness of *convex* federated optimization. More specifically, we perform several rounds of "*bootstrap*" FedAvg to learn features before solving a convexified version of the original optimization problem.

4.1 Computing the Empirical Neural Tangent Kernel

To sidestep the challenges presented by nonconvexity, we describe how we approximate a neural network by its "linearization." Given a neural network $f(\,\cdot\,;\theta_0)$ with weights $\theta_0 \in \mathbb{R}^P$ mapping inputs $x \in \mathbb{R}^D$ to $\mathbb{R}^C$, we replace it by its *empirical neural tangent kernel (eNTK)* approximation at θ_0 given by

$$f(x;\theta) \approx f(x;\theta_0) + (\theta - \theta_0)^\top \frac{\partial}{\partial\theta} f(x;\theta_0),$$

at each $x \in \mathbb{R}^D$. Under this approximation, $f(x;\theta)$ is a linear function of the "feature vector" $(f(x;\theta_0), \frac{\partial}{\partial\theta} f(x;\theta_0))$ and the original nonconvex optimization problem becomes (convex) linear regression with respect to these features.[2] Leveraging NTK for solving federated optimization problems has also been studied in previous work [29, 82].

To reduce the computational burden of working with the eNTK approximation, we make two further approximations: First, we randomly reinitialize the last layer of θ_0 and only consider $\frac{\partial}{\partial\theta} f(x;\theta_0)$ with respect to a single output logit. Over the randomness of this reinitialization, $\mathbb{E}[f(x;\theta_0)] = 0$. Moreover, given the random reinitialization, all the output logits of $f(x;\theta_0)$ are symmetric. These observations mean each data point x can be represented by a P-dimensional feature vector $\frac{\partial}{\partial\theta} f_1(x;\theta_0)$, where $f_1(\,\cdot\,;\theta_0)$ refers to the first output logit. Then, we apply a dimensionality reduction by subsampling p random coordinates from this P-dimensional featurization.[3] In our setting, this sub-sampling has the added benefit of reducing the number of bits communicated per round.

In summary, we transform our original (nonconvex) optimization problem over a neural network initialized at θ_0 into a convex optimization problem in three steps: (i) reinitialize the last layer of θ_0; (ii) for each data point x, compute the gradient $\phi_{\mathrm{eNTK}}(x;\theta_0) := \frac{\partial}{\partial\theta} f_1(x;\theta_0)$; (iii) subsample the coordinates of $\phi_{\mathrm{eNTK}}(x;\theta_0)$ for each x to obtain a reduced-dimensionality eNTK representation. Let $\mathcal{S}\colon \mathbb{R}^P \to \mathbb{R}^p$ denote this subsampling operation. Finally, we solve the resulting linear regression problem over these eNTK representations.[4]

4.2 Convexifying Federated Learning via eNTK Representations

The eNTK approximation lets us convexify the neural net optimization problem: following Section 4.1, we may extract (from a model trained with FedAvg) eNTK representations of inputs from each client. It remains to fit an overparameterized linear model using these eNTK features in a federated manner. For ease of presentation, we denote the subsampled eNTK representation of input x by $z \in \mathbb{R}^p$, where p is the eNTK feature dimension after subsampling. We use z_i^k to represent the eNTK feature of the i-th sample from the k-th client. Then, for K the number of clients, Y_i^k the one-hot encoded labels, n_k the number of data points of the k-th client, $n := \sum_{k\in[K]} n_k$ the number of data points across all clients, and $p_k := n_k/n$, we can approximate the nonconvex neural net optimization problem by the convex linear regression problem

$$\min_W L(W) := \sum_{k=1}^{K} p_k \cdot L_k(W), \qquad \text{where} \quad L_k(W) := \frac{1}{n_k}\sum_{i=1}^{n_k} \|W^\top z_i^k - Y_i^k\|_2^2. \tag{1}$$

To obtain the eNTK representation z of an input x, we take θ_0 in Section 4.1 to be the weights of a model trained with FedAvg. As we will show in Section 5, the convex reformulation in Eq. (1) significantly reduces the number of communication rounds needed to find an optimal solution.

[2]For classification problems, we one-hot encoded labels and fit a linear model using squared loss.

[3]That such representations empirically have low effective dimension due to fast eigenvalue decay [see, e.g., 75] means that such a random projection approximately preserves the geometry of the data points [5, 83]. For all of our experiments, we set $p = 100,000$.

[4]Given a fitted linear model with weights $W \in \mathbb{R}^{p\times C}$, the prediction at x is $\arg\max_j [W^\top \mathcal{S}(\phi_{\mathrm{eNTK}}(x))]_j$.

4.3 Train-Convexify-Train (TCT)

We now present our algorithm train-convexify-train (TCT), with convexification done via the neural tangent kernel, for federated optimization.

TCT — train-convexify-train with eNTK representations

- **Stage 1:** *Extract eNTK features from a FedAvg-trained model.* FedAvg is first used to train the model for T_1 communication rounds. Let θ_{T_1} denote the model weights after these T_1 rounds. Then, each client locally computes subsampled eNTK features, i.e., $z_i^k = \mathcal{S}(\phi_{\text{eNTK}}(x_i^k; \theta_{T_1}))$ for $k \in [K]$ and $i \in [n_k]$.
- **Stage 2:** *Decentralized linear regression with gradient correction.* Given samples $\{(z_i^k, Y_i^k)\}_{i=1}^{n_k}$ on each client k, first normalize the eNTK inputs of all clients with a single communication round.[a] Then, solve the linear regression problem defined in Eq. (1) by SCAFFOLD with local learning rate η and local steps M.[b]

[a]For every feature in the eNTK representation, subtract the mean and scale to unit variance.

[b]The detailed description of SCAFFOLD for solving linear regression problems can be found in Algorithm 1, Appendix A. It has the same communication and computation cost as FedAvg.

To motivate TCT, recall that in Section 3 we found that FedAvg learns "useful" features despite its poor performance, especially in the earlier layers. By taking an eNTK approximation, TCT optimizes a convex approximation while using information from *all* layers of the model. Empirically, we find that these extracted eNTK features significantly reduce the number of communication rounds needed to learn a performant model, even with data heterogeneity.

5 Experiments

We now study the performance of TCT for the decentralized training of deep neural networks in the presence of data heterogeneity. We compare TCT to state-of-the-art federated learning algorithms on three benchmark tasks in federated learning. For each task, we apply these algorithms on client data distributions with varying degrees of data heterogeneity. We find that our proposed approach significantly outperforms existing algorithms when clients have highly heterogeneous data across all tasks. For additional experimental results and implementation details, see Appendix B. Our code is available at `https://github.com/yaodongyu/TCT`.

5.1 Experimental Setup

Datasets and degrees of data heterogeneity. We assess the performance of federated learning algorithms on the image classification tasks FMNIST [80], CIFAR10, and CIFAR100 [41]. FMNIST and CIFAR10 each consist of 10 classes, while CIFAR100 includes images from 100 classes. There are 60,000 training images in FMNIST, and 50,000 training images in CIFAR10/100.

To vary the degree of data heterogeneity, we follow the setup of Li et al. [45]. We consider two types of non-i.i.d. data distribution: *(i) Data heterogeneity sampled from a symmetric Dirichlet distribution with parameter* α [49, 71]. That is, we sample $p_c \sim \text{Dir}_K(\alpha)$ from a K-dimensional symmetric Dirichlet distribution and assign a p_c^k-fraction of the class c samples to client k. (Smaller α corresponds to more heterogeneity.) *(ii) Clients get samples from a fixed subset of classes* [53]. That is, each client is allocated a subset of classes; then, the samples of each class are split into non-overlapping subsets and assigned to clients that were allocated this class. We use `#C` to denote the number of classes allocated to each client. For example, `#C=2` means each client has samples from 2 classes. To allow for consistent comparisons, all of our experiments are run with 10 clients.

Models. For FMNIST, we use a convolutional neural network with ReLU activations consisting of two convolutional layers with max pooling followed by two fully connected layers (SimpleCNN). For CIFAR10 and CIFAR100, we mainly consider an 18-layer residual network [25] with 4 basic residual blocks (ResNet-18). In Appendix B.2, we present experimental results for other architectures.

Algorithms and training schemes. We compare TCT to state-of-the-art federated learning algorithms, focusing on the widely-used algorithms FedAvg [53], FedProx [48], and SCAFFOLD [39].

Table 2: The top-1 accuracy (%) of our algorithm (TCT) vs. state-of-the-art federated learning algorithms evaluated on FMNIST, CIFAR10, and CIFAR100. We vary the degree of data heterogeneity by controlling the α parameter of the symmetric Dirichlet distribution $\mathrm{Dir}_K(\alpha)$ and the `#C` parameter for assigning how many labels each client owns. Higher accuracy is better. The highest top-1 accuracy in each setting is highlighted in **bold**.

Datasets	**Architectures**	**Methods**	**Non-i.i.d. degree**			
			`#C` $= 1$	`#C` $= 2$	$\alpha = 0.1$	$\alpha = 0.5$
FMNIST	SimpleCNN	FedAvg	35.10%	85.18%	86.18%	90.09%
		FedProx	50.04%	84.91%	86.31%	89.77%
		SCAFFOLD	12.80%	42.80%	83.87%	89.40%
		TCT	**86.32%**	**90.33%**	**90.78%**	**91.13%**
		Centralized	91.40%			
			`#C` $= 1$	`#C` $= 2$	$\alpha = 0.1$	$\alpha = 0.5$
CIFAR-10	ResNet-18	FedAvg	11.27%	56.86%	82.60%	90.43%
		FedProx	12.30%	56.87%	83.31%	90.68%
		SCAFFOLD	10.00%	46.75%	80.46%	90.72%
		TCT	**49.92%**	**83.02%**	**89.21%**	**91.10%**
		Centralized	91.90%			
			$\alpha = 0.001$	$\alpha = 0.01$	$\alpha = 0.1$	$\alpha = 0.5$
CIFAR-100	ResNet-18	FedAvg	53.89%	54.22%	63.49%	67.65%
		FedProx	52.87%	54.32%	63.47%	67.54%
		SCAFFOLD	49.86%	54.07%	65.67%	**71.07%**
		TCT	**68.42%**	**69.07%**	**69.66%**	69.68%
		Centralized	73.61%			

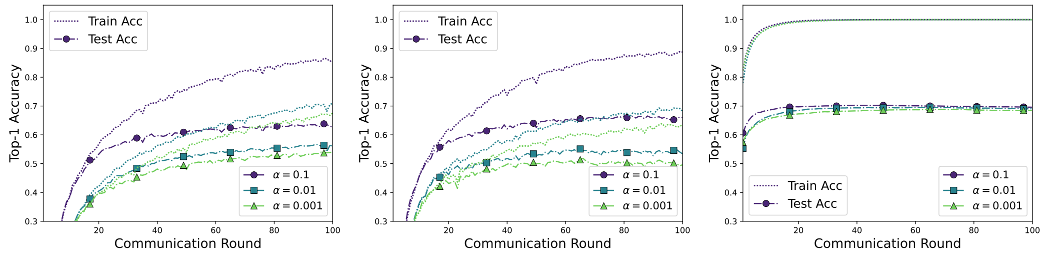

(a) FedAvg. (b) SCAFFOLD. (c) TCT.

Figure 2: Training/test accuracy vs. communication round for FedAvg (left), SCAFFOLD (middle), and our algorithm TCT (right) on the CIFAR100 dataset with various degrees of non-iid-ness ($\mathrm{Dir}_K(\alpha)$ with $\alpha \in \{0.1, 0.01, 0.001\}$). Dotted lines represent the training accuracy, and dashdot lines with markers represent the test accuracy.

(For comparisons to additional algorithms, see Appendix B.1.) Each client uses SGD with weight decay 10^{-5} and batch size 64 by default. For each baseline method, we run it for 200 total communication rounds using 5 local training epochs with local learning rate selected from $\{0.1, 0.01, 0.001\}$ by grid search. For TCT, we run 100 rounds of FedAvg in Stage 1 following the above and use 100 communication rounds in Stage 2 with $M = 500$ local steps and local learning rate $\eta = 5 \cdot 10^{-5}$.

5.2 Main Results

Table 2 displays the top-1 accuracy of all algorithm on the three tasks with varying degrees of data heterogeneity. We evaluated each algorithms on each task under four degrees of data heterogeneity. Smaller `#C` and α in Table 2 correspond to higher heterogeneity.

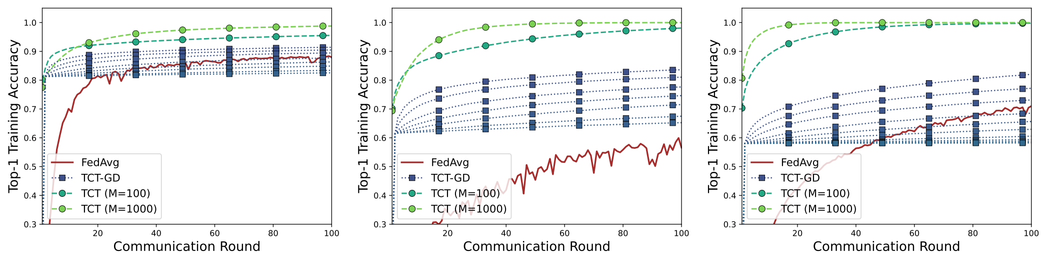

(a) FMNIST. (b) CIFAR10. (c) CIFAR100.

Figure 3: Training accuracy vs. communication round for full batch gradient descent (GD) and TCT on FMNIST-[#C=2] **(a)**, CIFAR10-[#C=2] **(b)**, and CIFAR100-[$\alpha = 0.01$] **(c)**. Each dotted line with square markers represents the training accuracy of GD with some learning rate. Dashed lines with circle markers represent the training accuracy of TCT with different numbers of local steps. We also include the training accuracy results of FedAvg with learning rate $\eta = 0.1$. We use TCT-GD to denote the variant of TCT which replaces SCAFFOLD with GD in Stage 2.

We find that the existing federated algorithms all suffer when data heterogeneity is high across all three tasks. For example, the top-1 accuracy of FedAvg on CIFAR-10 is 56.86% when #C=2, which is much worse than the 90.43% achieved in a more homogeneous setting (e.g. $\alpha = 0.5$). In contrast, TCT achieves consistently strong performance, even in the face of high data heterogeneity. More specifically, TCT achieves the best top-1 accuracy performance across all settings except CIFAR-100 with $\alpha = 0.5$, where TCT does only slightly worse than SCAFFOLD.

In absolute terms, we find that TCT is not affected much by data heterogeneity, with performance dropping by less than 1.5% on CIFAR100 as α goes from 0.5 to 0.001. Moreover, our algorithm improves over existing methods by at least 15% in the challenging cases, including FMNIST with #C=1, CIFAR-10 with #C=1 and #C=2, and CIFAR-100 with $\alpha = 0.01$ and $\alpha = 0.001$. And, perhaps surprisingly, our algorithm still performs relatively well in the extreme non-i.i.d. setting where each client sees only a single class.

Figure 2 compares the performances of FedAvg, SCAFFOLD, and TCT in more detail on CIFAR100 dataset with different degrees of data heterogeneity. We consider the Dirichlet distribution with parameter $\alpha \in \{0.1, 0.01, 0.001\}$ and compare the training and test accuracy of these three algorithms. As shown in Figures 2(a) and 2(b), both FedAvg and SCAFFOLD struggle when data heterogeneity is high: for both algorithms, test accuracy drops significantly when α decreases. In contrast, we see from Figure 2(c) that TCT maintains almost the same test accuracy for different α. Furthermore, the same set of default parameters for our algorithm, including local learning rate and the number of local steps, is relatively robust to different levels of data heterogeneity.

5.3 Communication Efficiency

To understand the effectiveness of the local steps in our algorithm, we compare SCAFFOLD (used in TCT-Stage 2) to full batch gradient descent (GD) applied to the overparameterized linear regression problem in Stage 2 of TCT on these datasets. For our algorithm, we set local steps $M \in \{10^2, 10^3\}$ and use the default local learning rate. For full batch GD, we vary the learning rate from 10^{-5} to 10^{-1} and visualize the ones that do not diverge.

The results are summarized in Figure 3. Each dotted line with square markers in Figure 3 corresponds to full batch GD with some learning rate. Across all three datasets, our proposed algorithm consistently outperforms full batch GD. Meanwhile, we find that more local steps for our algorithms lead to faster convergence across all settings. In particular, our algorithm converges within 20 communication rounds on CIFAR100 (as shown in Figure 3(c)). These results suggest that our proposed algorithm can largely leverage the local computation and improve communication efficiency.

5.4 Ablations

Gradient correction. We investigate the role of gradient correction when solving overparameterized linear regression with eNTK features in TCT. We compare SCAFFOLD (used in TCT) to FedAvg on solving the regression problems and summarize the results in Figure 4. We use the default

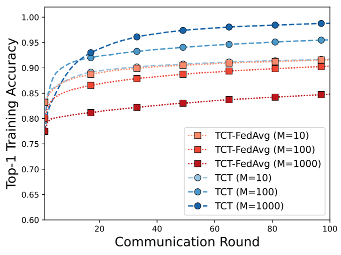

(a) FMNIST.

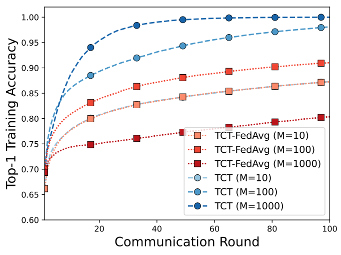

(b) CIFAR10.

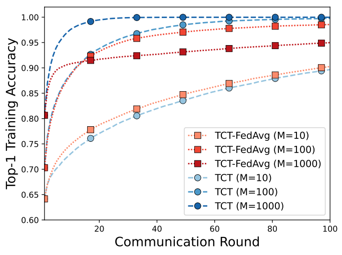

(c) CIFAR100.

Figure 4: Comparing TCT to TCT-FedAvg for solving the overparameterized linear regression problem on **(a)** FMNIST-[#C=2], **(b)** CIFAR10-[#C=2], and **(c)** CIFAR100-[$\alpha = 0.01$]. We use TCT-FedAvg to denote a variant of TCT that uses FedAvg instead of SCAFFOLD to perform linear regression in TCT-Stage 2. Dotted red lines with square markers represent the training accuracy of TCT-FedAvg with different numbers of local steps. Dashed blue red lines with circle markers represent the training accuracy of TCT with different numbers of local steps. A darker color means more local steps.

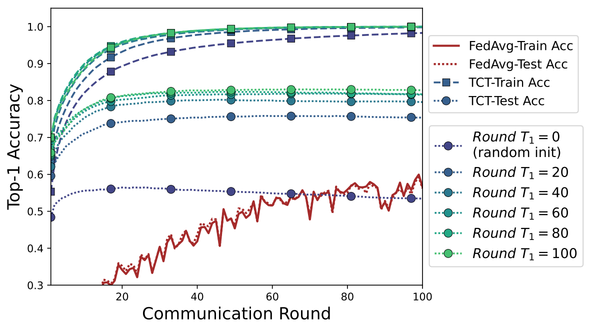

(a) Effect of FedAvg communication rounds in Stage 1.

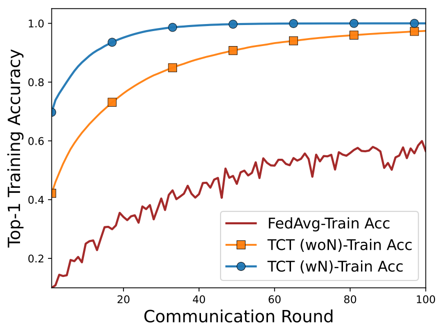

(b) Effect of normalization.

Figure 5: **(a).** We evaluate TCT on using checkpoints save at different communication rounds T_1 in Stage 1. $T_1 = 0$ corresponds to the randmon initialized model weights scenario (without FedAvg training). Dash lines with square markers represent the training accuracy, and dotted lines with circle makers represent the test accuracy. **(b).** We study the effect of pre-conditioning on TCT. TCT (wN) corresponds to the setting where eNTK features are normalized, and TCT (woN) corresponds to the without normalization step setting.

local learning rate and consider three different numbers of local steps for both algorithms, i.e., $M \in \{10, 100, 1000\}$. As shown in Figure 4, our approach largely outperforms FedAvg when the number of local steps is large ($M \geq 100$) across three datasets. We also find that the performance of FedAvg can even degrade when the number of local steps increases. For example, FedAvg with $M = 1000$ performs the worst across all three datasets. In contrast to FedAvg, SCAFFOLD converges faster when the number of local steps increases. These observations highlight the importance of gradient correction in our algorithm.

Model weights for computing eNTK features. To understand the impact of the model weights trained in Stage 1 of TCT, we evaluate TCT run with different T_1 parameters. We consider $T_1 \in \{0, 20, 40, 60, 80, 100\}$, where $T_1 = 0$ corresponds to randomly initialized weights. From Figure 5(a), we find that weights after FedAvg training are much more effective than weights at random initialization. Specifically, without FedAvg training, the eNTK (at random initialization) performs worse than standard FedAvg. In contrast, TCT significantly outperforms FedAvg by a large margin (roughly 20% in test accuracy) when eNTK features are extracted from a FedAvg-trained model. Also, we find that TCT is stable with respect to the choice of communication rounds T_1 in Stage 1. For example, models trained by TCT with $T_1 \geq 60$ achieve similar performance.

Effect of normalization. In Figure 5(b), we investigate the role of normalization on TCT by comparing TCT run with normalized and unnormalized eNTK features. The same number of local steps ($M = 500$) is applied for both settings. We tune the learning rate η for each setting and plot the run that performs best (as measured in training accuracy). The results in Figure 5(b) suggest that the normalization step in TCT significantly improves the communication efficiency by increasing convergence speed. In particular, TCT with normalization converges to nearly 100% training accuracy in approximately 40 communication rounds, which is much faster than TCT without normalization.

Pre-training vs. Bootstrapping. In Appendix B.4, we explore the effect of starting from a pre-trained model instead of relying on bootstrapping to learn the features. We find that pre-training further improves the performance of TCT and completely erases the gap between centralized and federated learning.

Additionally, we conduct experiments on investigating the role of training loss function and subsampling approximation in TCT-Stage 2. For TCT-Stage 2, we find that neither using the cross-entropy loss as the training objective nor applying full eNTK representations significantly improves the performance of TCT. On the other hand, applying subsampling approximation in TCT-Stage 2 can largely improve the communication efficiency compared to the full eNTK representations approach. See Appendix B.7 for detailed experimental results.

6 Conclusion

We have argued that nonconvexity poses a significant challenge for federated learning algorithms. We found that a neural network trained in such a manner does learn useful features, but fails to use them and thus has poor overall accuracy. To sidestep this issue, we proposed a *train-convexify-train* procedure: first, train the neural network using FedAvg; then, optimize (using SCAFFOLD) a convex approximation of the model obtained using its empirical neural tangent kernel. We showed that the first stage extracts meaningful features, whereas the second stage learns to utilize these features to obtain a highly performant model. The resulting algorithm is significantly faster and more stable to hyper-parameters than previous federated learning methods. Finally, we also showed that given a good pre-pretrained feature extractor, our convexify-train procedure fully closes the gap between centralized and federated learning.

Our algorithm adds to the growing body of work using eNTK to *linearize* neural networks and obtain tractable convex approximations. However, unlike most of these past works which only work with pre-trained models, our bootstrapping allows training models from scratch. Finally, we stress that the success of our approach underscores the need to revisit theoretical understanding of heterogeneous federated learning. Nonconvexity seems to play an outsized role but its effect in FL has hitherto been unexplored. In particular, black-box notions of difficulty such as gradient dissimilarity or distances between client optima seem insufficient to capture practical performance. It is likely that further progress in the field (e.g. federated pre-training of foundational models), will require tackling the issue of nonconvexity head on.

Acknowledgments and Disclosure of Funding

We would like to thank the anonymous reviewers for their constructive suggestions and comments. Yaodong Yu acknowledges support from the joint Simons Foundation-NSF DMS grant #2031899. Alexander Wei acknowledges support from an NSF Graduate Research Fellowship under grant DGE2146752. Sai Praneeth Karimireddy acknowledges support of an SNSF postdoc mobility fellowship. Yi Ma acknowledges support from ONR grants N00014-20-1-2002 and N00014-22-1-2102 and the joint Simons Foundation-NSF DMS grant #2031899. Michael Jordan acknowledges support of the ONR Mathematical Data Science program.

References

[1] Durmus Alp Emre Acar, Yue Zhao, Ramon Matas, Matthew Mattina, Paul Whatmough, and Venkatesh Saligrama. Federated learning based on dynamic regularization. In *International Conference on Learning Representations*, 2021. URL https://openreview.net/forum?id=B7v4QMR6Z9w.

[2] Alessandro Achille, Aditya Golatkar, Avinash Ravichandran, Marzia Polito, and Stefano Soatto. Lqf: Linear quadratic fine-tuning. In *Proceedings of the IEEE/CVF Conference on Computer Vision and Pattern Recognition*, pages 15729–15739, 2021.

[3] Andrei Afonin and Sai Praneeth Karimireddy. Towards model agnostic federated learning using knowledge distillation. *arXiv preprint arXiv:2110.15210*, 2021.

[4] Dan Alistarh, Demjan Grubic, Jerry Li, Ryota Tomioka, and Milan Vojnovic. QSGD: Communication-efficient SGD via gradient quantization and encoding. *Advances in Neural Information Processing Systems*, 30, 2017.

[5] Haim Avron, Kenneth L. Clarkson, and David P. Woodruff. Sharper bounds for regularized data fitting. In *Approximation, Randomization, and Combinatorial Optimization. Algorithms and Techniques, .*

[6] Eugene Bagdasaryan, Andreas Veit, Yiqing Hua, Deborah Estrin, and Vitaly Shmatikov. How to backdoor federated learning. In *International Conference on Artificial Intelligence and Statistics*, pages 2938–2948. PMLR, 2020.

[7] Peva Blanchard, El Mahdi El Mhamdi, Rachid Guerraoui, and Julien Stainer. Machine learning with adversaries: Byzantine tolerant gradient descent. *Advances in Neural Information Processing Systems*, 30, 2017.

[8] Kallista Bonawitz, Peter Kairouz, Brendan McMahan, and Daniel Ramage. Federated learning and privacy: Building privacy-preserving systems for machine learning and data science on decentralized data. *Queue*, 19(5):87–114, 2021.

[9] Keith Bonawitz, Vladimir Ivanov, Ben Kreuter, Antonio Marcedone, H Brendan McMahan, Sarvar Patel, Daniel Ramage, Aaron Segal, and Karn Seth. Practical secure aggregation for privacy-preserving machine learning. In *Proceedings of the 2017 ACM SIGSAC Conference on Computer and Communications Security*, pages 1175–1191, 2017.

[10] Keith Bonawitz, Hubert Eichner, Wolfgang Grieskamp, Dzmitry Huba, Alex Ingerman, Vladimir Ivanov, Chloe Kiddon, Jakub Konečnỳ, Stefano Mazzocchi, Brendan McMahan, et al. Towards federated learning at scale: System design. *Proceedings of Machine Learning and Systems*, 1: 374–388, 2019.

[11] Zachary Charles, Zachary Garrett, Zhouyuan Huo, Sergei Shmulyian, and Virginia Smith. On large-cohort training for federated learning. *Advances in Neural Information Processing Systems*, 34, 2021.

[12] El Mahdi Chayti and Sai Praneeth Karimireddy. Optimization with access to auxiliary information. *arXiv preprint arXiv:2206.00395*, 2022.

[13] Liam Collins, Hamed Hassani, Aryan Mokhtari, and Sanjay Shakkottai. Exploiting shared representations for personalized federated learning. In *International Conference on Machine Learning*, pages 2089–2099. PMLR, 2021.

[14] Jeffrey Dean, Greg Corrado, Rajat Monga, Kai Chen, Matthieu Devin, Mark Mao, Marc'aurelio Ranzato, Andrew Senior, Paul Tucker, Ke Yang, et al. Large scale distributed deep networks. *Advances in Neural Information Processing Systems*, 25, 2012.

[15] Aaron Defazio, Francis Bach, and Simon Lacoste-Julien. Saga: A fast incremental gradient method with support for non-strongly convex composite objectives. *Advances in Neural Information Processing Systems*, 27, 2014.

[16] Yuyang Deng, Mohammad Mahdi Kamani, and Mehrdad Mahdavi. Adaptive personalized federated learning. *arXiv preprint arXiv:2003.13461*, 2020.

[17] Jean Ogier du Terrail, Samy-Safwan Ayed, Edwige Cyffers, Felix Grimberg, Chaoyang He, Regis Loeb, Paul Mangold, Tanguy Marchand, Othmane Marfoq, Erum Mushtaq, et al. Flamby: Datasets and benchmarks for cross-silo federated learning in realistic settings. 2022.

[18] Alireza Fallah, Aryan Mokhtari, and Asuman Ozdaglar. Personalized federated learning: A meta-learning approach. *arXiv preprint arXiv:2002.07948*, 2020.

[19] Minghong Fang, Xiaoyu Cao, Jinyuan Jia, and Neil Gong. Local model poisoning attacks to {Byzantine-Robust} federated learning. In *29th USENIX Security Symposium (USENIX Security 20)*, pages 1605–1622, 2020.

[20] Stanislav Fort, Gintare Karolina Dziugaite, Mansheej Paul, Sepideh Kharaghani, Daniel M Roy, and Surya Ganguli. Deep learning versus kernel learning: an empirical study of loss landscape geometry and the time evolution of the neural tangent kernel. In *Advances in Neural Information Processing Systems*, volume 33, pages 5850–5861, 2020.

[21] Clement Fung, Chris JM Yoon, and Ivan Beschastnikh. Mitigating sybils in federated learning poisoning. *arXiv preprint arXiv:1808.04866*, 2018.

[22] Micah Goldblum, Jonas Geiping, Avi Schwarzschild, Michael Moeller, and Tom Goldstein. Truth or backpropaganda? an empirical investigation of deep learning theory. *arXiv preprint arXiv:1910.00359*, 2019.

[23] Priya Goyal, Piotr Dollár, Ross Girshick, Pieter Noordhuis, Lukasz Wesolowski, Aapo Kyrola, Andrew Tulloch, Yangqing Jia, and Kaiming He. Accurate, large minibatch SGD: Training Imagenet in 1 hour. *arXiv preprint arXiv:1706.02677*, 2017.

[24] Farzin Haddadpour, Mohammad Mahdi Kamani, Aryan Mokhtari, and Mehrdad Mahdavi. Federated learning with compression: Unified analysis and sharp guarantees. In *International Conference on Artificial Intelligence and Statistics*, pages 2350–2358. PMLR, 2021.

[25] Kaiming He, Xiangyu Zhang, Shaoqing Ren, and Jian Sun. Deep residual learning for image recognition. In *Proceedings of the IEEE conference on computer vision and pattern recognition*, pages 770–778, 2016.

[26] Lie He, Sai Praneeth Karimireddy, and Martin Jaggi. Byzantine-robust decentralized learning via self-centered clipping. *arXiv preprint arXiv:2202.01545*, 2022.

[27] Kevin Hsieh, Amar Phanishayee, Onur Mutlu, and Phillip Gibbons. The non-iid data quagmire of decentralized machine learning. In *International Conference on Machine Learning*, pages 4387–4398. PMLR, 2020.

[28] Tzu-Ming Harry Hsu, Hang Qi, and Matthew Brown. Measuring the effects of non-identical data distribution for federated visual classification. *arXiv preprint arXiv:1909.06335*, 2019.

[29] Baihe Huang, Xiaoxiao Li, Zhao Song, and Xin Yang. Fl-ntk: A neural tangent kernel-based framework for federated learning analysis. In *International Conference on Machine Learning*, pages 4423–4434. PMLR, 2021.

[30] Like Hui and Mikhail Belkin. Evaluation of neural architectures trained with square loss vs cross-entropy in classification tasks. *arXiv preprint arXiv:2006.07322*, 2020.

[31] Forrest N Iandola, Matthew W Moskewicz, Khalid Ashraf, and Kurt Keutzer. Firecaffe: near-linear acceleration of deep neural network training on compute clusters. In *Proceedings of the IEEE Conference on Computer Vision and Pattern Recognition*, pages 2592–2600, 2016.

[32] Sergey Ioffe and Christian Szegedy. Batch normalization: Accelerating deep network training by reducing internal covariate shift. In *International conference on machine learning*, pages 448–456. PMLR, 2015.

[33] Pavel Izmailov, Dmitrii Podoprikhin, Timur Garipov, Dmitry Vetrov, and Andrew Gordon Wilson. Averaging weights leads to wider optima and better generalization. *arXiv preprint arXiv:1803.05407*, 2018.

[34] Arthur Jacot, Franck Gabriel, and Clément Hongler. Neural tangent kernel: Convergence and generalization in neural networks. *Advances in Neural Information Processing Systems*, 31, 2018.

[35] Rie Johnson and Tong Zhang. Accelerating stochastic gradient descent using predictive variance reduction. *Advances in Neural Information Processing Systems*, 26, 2013.

[36] Charles I Jones and Christopher Tonetti. Nonrivalry and the economics of data. *American Economic Review*, 110(9):2819–58, 2020.

[37] Peter Kairouz, H. Brendan McMahan, et al. Advances and open problems in federated learning. *Foundations and Trends® in Machine Learning*, 14(1–2):1–210, 2021.

[38] Sai Praneeth Karimireddy, Martin Jaggi, Satyen Kale, Mehryar Mohri, Sashank J Reddi, Sebastian U Stich, and Ananda Theertha Suresh. Mime: Mimicking centralized stochastic algorithms in federated learning. *arXiv preprint arXiv:2008.03606*, 2020.

[39] Sai Praneeth Karimireddy, Satyen Kale, Mehryar Mohri, Sashank Reddi, Sebastian Stich, and Ananda Theertha Suresh. Scaffold: Stochastic controlled averaging for federated learning. In *International Conference on Machine Learning*, pages 5132–5143. PMLR, 2020.

[40] Sai Praneeth Karimireddy, Lie He, and Martin Jaggi. Byzantine-robust learning on heterogeneous datasets via bucketing. In *International Conference on Learning Representations*, 2021.

[41] Alex Krizhevsky, Geoffrey Hinton, et al. Learning multiple layers of features from tiny images. 2009.

[42] Viraj Kulkarni, Milind Kulkarni, and Aniruddha Pant. Survey of personalization techniques for federated learning. In *2020 Fourth World Conference on Smart Trends in Systems, Security and Sustainability (WorldS4)*, pages 794–797. IEEE, 2020.

[43] Bogdan Kulynych, David Madras, Smitha Milli, Inioluwa Deborah Raji, Angela Zhou, and Richard Zemel. Participatory approaches to machine learning. International Conference on Machine Learning Workshop, 2020.

[44] Jaehoon Lee, Lechao Xiao, Samuel Schoenholz, Yasaman Bahri, Roman Novak, Jascha Sohl-Dickstein, and Jeffrey Pennington. Wide neural networks of any depth evolve as linear models under gradient descent. *Advances in Neural Information Processing Systems*, 32, 2019.

[45] Qinbin Li, Yiqun Diao, Quan Chen, and Bingsheng He. Federated learning on non-iid data silos: An experimental study. *arXiv preprint arXiv:2102.02079*, 2021.

[46] Qinbin Li, Bingsheng He, and Dawn Song. Model-contrastive federated learning. In *Proceedings of the IEEE/CVF Conference on Computer Vision and Pattern Recognition*, pages 10713–10722, 2021.

[47] Tian Li, Maziar Sanjabi, Ahmad Beirami, and Virginia Smith. Fair resource allocation in federated learning. *arXiv preprint arXiv:1905.10497*, 2019.

[48] Tian Li, Anit Kumar Sahu, Manzil Zaheer, Maziar Sanjabi, Ameet Talwalkar, and Virginia Smith. Federated optimization in heterogeneous networks. *Proceedings of Machine Learning and Systems*, 2:429–450, 2020.

[49] Tao Lin, Lingjing Kong, Sebastian U Stich, and Martin Jaggi. Ensemble distillation for robust model fusion in federated learning. *Advances in Neural Information Processing Systems*, 33: 2351–2363, 2020.

[50] Tao Lin, Sai Praneeth Karimireddy, Sebastian U Stich, and Martin Jaggi. Quasi-global momentum: Accelerating decentralized deep learning on heterogeneous data. *arXiv preprint arXiv:2102.04761*, 2021.

[51] Philip M Long. Properties of the after kernel. *arXiv preprint arXiv:2105.10585*, 2021.

[52] Lingjuan Lyu, Han Yu, and Qiang Yang. Threats to federated learning: A survey. *arXiv preprint arXiv:2003.02133*, 2020.

[53] Brendan McMahan, Eider Moore, Daniel Ramage, Seth Hampson, and Blaise Aguera y Arcas. Communication-efficient learning of deep networks from decentralized data. In *Artificial Intelligence and Statistics*, pages 1273–1282. PMLR, 2017.

[54] Konstantin Mishchenko, Grigory Malinovsky, Sebastian Stich, and Peter Richtárik. Proxskip: Yes! local gradient steps provably lead to communication acceleration! finally! *arXiv preprint arXiv:2202.09357*, 2022.

[55] Mehryar Mohri, Gary Sivek, and Ananda Theertha Suresh. Agnostic federated learning. In *International Conference on Machine Learning*, pages 4615–4625. PMLR, 2019.

[56] Viraaji Mothukuri, Reza M Parizi, Seyedamin Pouriyeh, Yan Huang, Ali Dehghantanha, and Gautam Srivastava. A survey on security and privacy of federated learning. *Future Generation Computer Systems*, 115:619–640, 2021.

[57] Fangzhou Mu, Yingyu Liang, and Yin Li. Gradients as features for deep representation learning. *arXiv preprint arXiv:2004.05529*, 2020.

[58] Kaan Ozkara, Navjot Singh, Deepesh Data, and Suhas Diggavi. Quped: Quantized personalization via distillation with applications to federated learning. *Advances in Neural Information Processing Systems*, 34, 2021.

[59] Alex Pentland, Alexander Lipton, and Thomas Hardjono. *Building the New Economy: Data as Capital*. MIT Press, 2021.

[60] Swaroop Ramaswamy, Om Thakkar, Rajiv Mathews, Galen Andrew, H Brendan McMahan, and Françoise Beaufays. Training production language models without memorizing user data. *arXiv preprint arXiv:2009.10031*, 2020.

[61] Sashank J. Reddi, Zachary Charles, Manzil Zaheer, Zachary Garrett, Keith Rush, Jakub Konečný, Sanjiv Kumar, and Hugh Brendan McMahan. Adaptive federated optimization. In *International Conference on Learning Representations*, 2021. URL https://openreview.net/forum?id=LkFG3lB13U5.

[62] Yuxin Shi, Han Yu, and Cyril Leung. A survey of fairness-aware federated learning. *arXiv preprint arXiv:2111.01872*, 2021.

[63] Sidak Pal Singh and Martin Jaggi. Model fusion via optimal transport. *Advances in Neural Information Processing Systems*, 33:22045–22055, 2020.

[64] Jinhyun So, Başak Güler, and A Salman Avestimehr. Byzantine-resilient secure federated learning. *IEEE Journal on Selected Areas in Communications*, 39(7):2168–2181, 2020.

[65] Sebastian U Stich and Sai Praneeth Karimireddy. The error-feedback framework: Better rates for sgd with delayed gradients and compressed updates. *Journal of Machine Learning Research*, 21:1–36, 2020.

[66] Ziteng Sun, Peter Kairouz, Ananda Theertha Suresh, and H Brendan McMahan. Can you really backdoor federated learning? *arXiv preprint arXiv:1911.07963*, 2019.

[67] Ananda Theertha Suresh, X Yu Felix, Sanjiv Kumar, and H Brendan McMahan. Distributed mean estimation with limited communication. In *International Conference on Machine Learning*, pages 3329–3337. PMLR, 2017.

[68] Yue Tan, Guodong Long, Lu Liu, Tianyi Zhou, Qinghua Lu, Jing Jiang, and Chengqi Zhang. Fedproto: Federated prototype learning over heterogeneous devices. *arXiv preprint arXiv:2105.00243*, 2021.

[69] Hongyi Wang, Kartik Sreenivasan, Shashank Rajput, Harit Vishwakarma, Saurabh Agarwal, Jy-yong Sohn, Kangwook Lee, and Dimitris Papailiopoulos. Attack of the tails: Yes, you really can backdoor federated learning. *Advances in Neural Information Processing Systems*, 33: 16070–16084, 2020.

[70] Jianyu Wang, Vinayak Tantia, Nicolas Ballas, and Michael Rabbat. Slowmo: Improving communication-efficient distributed sgd with slow momentum. *arXiv preprint arXiv:1910.00643*, 2019.

[71] Jianyu Wang, Qinghua Liu, Hao Liang, Gauri Joshi, and H Vincent Poor. Tackling the objective inconsistency problem in heterogeneous federated optimization. *Advances in Neural Information Processing Systems*, 33:7611–7623, 2020.

[72] Jianyu Wang, Zachary Charles, Zheng Xu, Gauri Joshi, H Brendan McMahan, Maruan Al-Shedivat, Galen Andrew, Salman Avestimehr, Katharine Daly, Deepesh Data, et al. A field guide to federated optimization. *arXiv preprint arXiv:2107.06917*, 2021.

[73] Jianyu Wang, Rudrajit Das, Gauri Joshi, Satyen Kale, Zheng Xu, and Tong Zhang. On the unreasonable effectiveness of federated averaging with heterogeneous data. *arXiv preprint arXiv:2206.04723*, 2022.

[74] Shiqiang Wang, Tiffany Tuor, Theodoros Salonidis, Kin K Leung, Christian Makaya, Ting He, and Kevin Chan. Adaptive federated learning in resource constrained edge computing systems. *IEEE Journal on Selected Areas in Communications*, 37(6):1205–1221, 2019.

[75] Alexander Wei, Wei Hu, and Jacob Steinhardt. More than a toy: Random matrix models predict how real-world neural representations generalize. *arXiv preprint arXiv:2203.06176*, 2022.

[76] Blake E Woodworth, Kumar Kshitij Patel, and Nati Srebro. Minibatch vs local sgd for heterogeneous distributed learning. *Advances in Neural Information Processing Systems*, 33:6281–6292, 2020.

[77] Mitchell Wortsman, Gabriel Ilharco, Samir Yitzhak Gadre, Rebecca Roelofs, Raphael Gontijo-Lopes, Ari S Morcos, Hongseok Namkoong, Ali Farhadi, Yair Carmon, Simon Kornblith, et al. Model soups: averaging weights of multiple fine-tuned models improves accuracy without increasing inference time. *arXiv preprint arXiv:2203.05482*, 2022.

[78] Qiong Wu, Kaiwen He, and Xu Chen. Personalized federated learning for intelligent IoT applications: A cloud-edge based framework. *IEEE Open Journal of the Computer Society*, 1: 35–44, 2020.

[79] Yuxin Wu and Kaiming He. Group normalization. In *Proceedings of the European Conference on Computer Vision (ECCV)*, pages 3–19, 2018.

[80] Han Xiao, Kashif Rasul, and Roland Vollgraf. Fashion-MNIST: a novel image dataset for benchmarking machine learning algorithms. *arXiv preprint arXiv:1708.07747*, 2017.

[81] Fuxun Yu, Weishan Zhang, Zhuwei Qin, Zirui Xu, Di Wang, Chenchen Liu, Zhi Tian, and Xiang Chen. Fed2: Feature-aligned federated learning. In *Proceedings of the 27th ACM SIGKDD Conference on Knowledge Discovery & Data Mining*, pages 2066–2074, 2021.

[82] Kai Yue, Richeng Jin, Ryan Pilgrim, Chau-Wai Wong, Dror Baron, and Huaiyu Dai. Neural tangent kernel empowered federated learning. In *International Conference on Machine Learning*, pages 25783–25803. PMLR, 2022.

[83] Luca Zancato, Alessandro Achille, Avinash Ravichandran, Rahul Bhotika, and Stefano Soatto. Predicting training time without training. *Advances in Neural Information Processing Systems*, 33:6136–6146, 2020.

Checklist

1. For all authors...
   (a) Do the main claims made in the abstract and introduction accurately reflect the paper's contributions and scope? [Yes]
   (b) Did you describe the limitations of your work? [Yes]
   (c) Did you discuss any potential negative societal impacts of your work? [Yes] Our work furthers the goal of federated learning which aims to make ML more participatory. We see this overall as a positive outcome. However, it can potentially also be used to circumvent existing data portability and privacy regulations. E.g. hospitals with previously confidential patient health records could circumvent privacy regulations by using FL. They can sell their information to an insurance company, without directly revealing any raw patient data. We believe preventing such bad outcomes requires direct regulatory measures (e.g. prohibiting insurance companies from discriminating among their consumers) are necessary rather than on relying on vague notions of privacy. More generally, laws and mechanisms need to be designed to ensure that companies don't capture all the benefits arising from the access to data through FL, and instead these benefits are passed on to all sections of society.
   (d) Have you read the ethics review guidelines and ensured that your paper conforms to them? [Yes]
2. If you are including theoretical results...
   (a) Did you state the full set of assumptions of all theoretical results? [N/A]
   (b) Did you include complete proofs of all theoretical results? [N/A]
3. If you ran experiments...
   (a) Did you include the code, data, and instructions needed to reproduce the main experimental results (either in the supplemental material or as a URL)? [Yes] See supplemental material.
   (b) Did you specify all the training details (e.g., data splits, hyperparameters, how they were chosen)? [Yes] See Section 5.1 and Appendix A.
   (c) Did you report error bars (e.g., with respect to the random seed after running experiments multiple times)? [Yes]
   (d) Did you include the total amount of compute and the type of resources used (e.g., type of GPUs, internal cluster, or cloud provider)? [Yes]
4. If you are using existing assets (e.g., code, data, models) or curating/releasing new assets...
   (a) If your work uses existing assets, did you cite the creators? [Yes]
   (b) Did you mention the license of the assets? [N/A]
   (c) Did you include any new assets either in the supplemental material or as a URL? [No]
   (d) Did you discuss whether and how consent was obtained from people whose data you're using/curating? [N/A]
   (e) Did you discuss whether the data you are using/curating contains personally identifiable information or offensive content? [N/A]
5. If you used crowdsourcing or conducted research with human subjects...
   (a) Did you include the full text of instructions given to participants and screenshots, if applicable? [N/A]
   (b) Did you describe any potential participant risks, with links to Institutional Review Board (IRB) approvals, if applicable? [N/A]
   (c) Did you include the estimated hourly wage paid to participants and the total amount spent on participant compensation? [N/A]

Appendix

A Additional Details About Our Algorithm

A.1 An Efficient Implementation of SCAFFOLD

Algorithm 1 Efficient implementation of SCAFFOLD

```
Input: losses $\{L_k\}$, $k \in [K]$. Number of local steps $M$, server model $\theta^0$, learning rate $\eta$.
Initialization: client corrections $\{h_k^{-1} = \mathbf{0}\}$, local models$\{\widehat{\theta}_i^0\} = \theta^0,\ k \in [K]$
for round $t = 0, 1, \ldots, T$ do
    for clients $k = 1, \ldots, K$ in parallel do
        Receive $\theta^t$ from server. Update correction
            $h_k^t = h_k^{t-1} + \frac{1}{M\eta}(\theta^t - \widehat{\theta}_k^t).$    (2)
        Initialize client local model $\widehat{\theta}_i^{t,0} = \theta^t$.
        for $m = 1, \ldots, M$ do
            Update with a stochastic gradient sampled from local client data
            $\widehat{\theta}_k^{t,m+1} = \widehat{\theta}_k^{t,m} - \eta\left(\nabla L_k(\theta_i^{t,m}; \xi_k^{t,m}) - h_k^t\right).$    (3)
        end for
        Set $\widehat{\theta}_k^{t+1} = \widehat{\theta}_k^{t,M+1}$. Communicate $\widehat{\theta}_k^{t+1}$ to server.
    end for
    Aggregate $\theta^{t+1} = \frac{1}{K}\sum_{k=1}^K \widehat{\theta}_k^{t+1}$.[5]
end for
```

We describe a more communication efficient implementation of SCAFFOLD which is equivalent to Option II of SCAFFOLD from [39]. Our implementation only requires a single model to be communicated between the client and server each round, making its communication complexity exactly equivalent to that of FedAvg. To see the equivalence, we prove that our implementation satisfies the following condition for any time step $t \geq 0$:

$$c_k^{t+1} := \frac{1}{M}\sum_{m\in[M]} \nabla L_k(\theta_k^{t,m}; \xi_k^{t,m}), \text{ and}$$

$$c^{t+1} := \frac{1}{K}\sum_{k\in[K]} c_k^t, \text{ we maintain the invariant that}$$

$$h_k^{t+1} = c_k^{t+1} - c^{t+1}.$$

To see this, note that the local client model after updating in round t is

$$\begin{aligned}\widehat{\theta}_k^{t+1} &= \widehat{\theta}_k^{t,M+1} \\ &= \theta^t - \eta\sum_{k\in[K]} \nabla L_k(\theta_k^{t,m}; \xi_k^{t,m}) - h_k^t \\ &= \theta^t - M\eta(c_k^{t+1} - h_k^t).\end{aligned}$$

By averaging this over the clients, we can see that the server model is

$$\theta^{t+1} = \theta^t - M\eta\Big(c^{t+1} - \frac{1}{K}\sum_{l\in[K]} h_l^t\Big).$$

[5]Note that when different clients have different number of data points, the actual aggregation step is $\theta^{t+1} = \sum_{k=1}^K ({n_k}/{\sum_j n_j})\widehat{\theta}_k^{t+1}$. However, we present the simplified version with equal weights for all clients to ease the comparison with the pseudocode in Karimireddy et al. [39].

By induction, suppose that $h_k^t = c_k^t - c^t$. This implies that summing over the clients, it becomes zero; i.e., $\sum_{l\in[K]} h_l^t = 0$. Plugging this and the previous computations, we have

$$\begin{aligned} h_k^{t+1} &= h_k^t + \tfrac{1}{M\eta}(\theta^{t+1} - \widehat{\theta}_k^{t+1}) \\ &= h_k^t + \tfrac{1}{M\eta}(-M\eta c^{t+1} + M\eta(c_k^{t+1} - h_k^t)) \\ &= c_k^{t+1} - c^{t+1} \,. \end{aligned}$$

For the base step at $t = 0$, note that $h_i^0 = \mathbf{0}$. This completes the proof by induction.

A.2 Additional Implementation Details

Algorithm 2 TCT: complete pseudo-code

```
**Input:** input dim $D$, output dim $C$, loss $\ell(\cdot,\cdot) : \mathbb{R}^{C\times C} \to \mathbb{R}$, aggr. weights $\{w_1, \ldots, w_K\}$,
model $f$ with parameters $\theta \in \mathbb{R}^P$: $f(x;\theta) = \phi \circ \omega\ (x) : \mathbb{R}^D \to \mathbb{R}^C$ (e.g., ResNet18), composed
of a feature extractor $\phi : \mathbb{R}^D \to \mathbb{R}^E$ and final linear layer $\omega : \mathbb{R}^E \to \mathbb{R}^C$.
**Hyper-parameters:** Local steps $M$ (default 500), Stage-1 lr $\eta_1$ (default 0.01), Stage-1 rounds $T_1$
(default 100), Stage-2 lr $\eta_2$ (default $5 \cdot 10^{-5}$), Stage-2 rounds $T_2$ (default 100).

**Stage 1 (Bootstrapping):**
Initialize server model $\theta^0$.
**for** round $t = 0, 1, \ldots, T_1$ **do**
  **for** clients $k = 1, \ldots, K$ in parallel **do**
    Receive $\theta^t$ from server and initialize client local model $\widehat{\theta}_k^{t,0} = \theta^t$.
    **for** $m = 1, \ldots, M$ **do**
      Update with a mini-batch gradient sampled from local client data $(x_k^{t,m}, y_k^{t,m})$
          $\widehat{\theta}_k^{t,m+1} = \widehat{\theta}_k^{t,m} - \eta_i \left(\nabla_\theta \ell(f(x_k^{t,m}; \theta_k^{t,m}), y_k^{t,m}) - h_k^t\right)$ .
    **end for**
    Communicate $\widehat{\theta}_k^{t+1}$ to server.
  **end for**
  Aggregate $\theta^{t+1} = \frac{1}{\sum_k w_k} \sum_{k=1}^K w_k \widehat{\theta}_k^{t+1}$ .
**end for**

**Stage 2 (Convexification):**
Input: Bootstrapped parameters $\theta^B$ decomposed as $\theta^B = \phi^B \circ \omega^B$.
Randomly re-initialize using fixed seed linear layer $\omega^r$ and define $\theta^0 := \phi^B \circ \omega^r$.
[Comment:] *Define basis vector* $\mathbf{e_1} := (1, 0, \ldots, 0)$. *For input* $x$, $(\mathbf{e}_1^\top f(x;\theta^0))$ *is the first logit.*
Optionally, compute a random sub-sampling mask $\mathcal{S}(\phi)$ over feature params using fixed seed .
[Comment:] *For a given input* $x$, *we will learn parameters* $(\varphi, b)$ *for prediction as*
    $\hat{y} = \varphi^\top \phi_{\text{eNTK}}(x) + b, \quad \text{where} \quad \phi_{\text{eNTK}}(x) := \mathcal{S}\left(\nabla_\phi(\mathbf{e}_1^\top f(x; \phi^B \circ \omega^r))\right)$ .

Compute normalized eNTK features $\tilde{\phi}_{\text{eNTK}}(x)$ (mean 0 and variance 1) across clients.
Also normalize targets to mean 0 using $\tilde{y} := y - \frac{1}{C}\mathbf{1}$.
Run SCAFFOLD (Algorithm 1) over params $\psi := (\varphi, b)$ with learning rate $\eta_2$, local steps $M$,
initial server params: $\psi^0 = \mathbf{0}$, and client losses $\{L_k\}$ defined over the local data as
    $L_k(\psi) := \sum_{(x_k, y_k)} \left(\varphi^\top \tilde{\phi}_{\text{eNTK}}(x_k) + b - \tilde{y}_k\right)^2$ .
```

Additional details about linear regression in TCT. In our experiments, we normalize the one-hot encoded label of each sample so that the normalized one-hot encoded label has mean 0. More specifically, we subtract $[1/C, \ldots, 1/C]^\top \in \mathbb{R}^{C\times 1}$ from the one-hot encoding label vector, where C is the number of classes. Further, Hui and Belkin [30] show that performance for large number

Algorithm 3 Compute eNTK Pseudocode, PyTorch-like

```
def compute_eNTK(model, X, num_params, subsample_size=100000, seed=123):
    """compute eNTK of input X with model"""
    # model: model for linearization
    # X: (n x d), n -- number of samples, d -- input dimension
    # subsample_size: parameter of subsampling operation
    # seed: random seed for subsampling operation
    # num_params: total number of parameters for model
    model.eval()
    params = list(model.parameters())
    torch.manual_seed(seed)
    torch.cuda.manual_seed(seed)
    random_index = torch.randperm(num_params)[:subsample_size]
    eNTKs = torch.zeros((X.size()[0], subsample_size))
    for i in range(X.size()[0]):
        # compute eNTK for the i-th input
        model.zero_grad()
        model.forward(X[i:i+1])[0].backward()
        eNTK = []
        for param in params:
            if param.requires_grad:
                eNTK.append(param.grad.flatten())
        eNTK = torch.cat(eNTK)
        # subsampling
        eNTKs[i, :] = eNTK[random_index]
    return eNTKs
```

of classes can be improved by increasing the penalty for mis-classification and scaling the target from 1 to a larger value (e.g., 30). Achille et al. [2] show that using Leaky-ReLU, and using K-FAC preconditioning further improves the performance. However, we do not explore such optimizations in this work–these (and other optimization tricks for least-squares regression) can be easily incorporated into our framework.

Local learning rate for TCT. From our experiments, we find that small local learning rates ($\eta \leq 10^{-4}$) achieve good train/test accuracy performance for TCT with the normalization step. When the normalization step in TCT is applied, larger local learning rates diverge. Meanwhile, local learning rates from $[10^{-6}, 10^{-4}]$ achieve similar performance for TCT (as shown in Table 8). On the other hand, without the normalization step, TCT with large learning rate ($\eta \in [0.01, 0.5]$) does not diverge. When running more communication rounds, TCT (without the normalization step) with large learning rate achieves similar performance as the default TCT (with the normalization step).

Additional details about Stage 2 of TCT. To solve the linear regression problem in TCT-**Stage 2**, we use the full batch gradient in Eq. (3) of Algorithm 1 in our implementation.

Additional details about Figure 5. We consider CIFAR10-[#C=2] in Figure 5(a) and 5(b).

Details about the total amount of compute. We use NVIDIA 2080 Ti, A4000, and A100 GPUs, and our experiments required around 500 hours of GPU time.

B Additional Experimental Results

B.1 Additional Baselines

In comparison with FedAdam and FedDyn. We compare TCT to FedAdam [61], FedDyn [1], and FedNova [71] in Table 3. We consider four settings in Table 3, including CIFAR10 (`#C` $= 2$), CIFAR10 ($\alpha = 0.1$), CIFAR100 ($\alpha = 0.001$), and CIFAR100 ($\alpha = 0.01$). For FedDyn, we perform similar hyperparameter selection as FedAvg; i.e., select local learning rate from $\{0.1, 0.01, 0.001\}$. For FedAdam, following recommendation by [61], we set the global learning rate as $\eta_{\text{global}} = 0.1$ and select local learning rate from $\{10^{-1}, 10^{-1.5}, 10^{-2}, 10^{-2.5}, 10^{-3}\}$. Similar to results in Table 2, we find that TCT significantly outperforms the existing methods in high data heterogeneity settings.

Table 3: The top-1 test accuracy ($\%$) of our algorithm (TCT) vs. other federated learning algorithms (FedAdam [61], FedDyn [1], and FedNova [71]) evaluated on CIFAR10 and CIFAR100. We vary the degree of data heterogeneity by controlling the α parameter of the symmetric Dirichlet distribution $\text{Dir}_K(\alpha)$ and the `#C` parameter for assigning how many labels each client owns. Higher accuracy is better. The highest top-1 accuracy in each setting is highlighted in **bold**.

Methods	Datasets			
	CIFAR10 (`#C` $= 2$)	CIFAR10 ($\alpha = 0.1$)	CIFAR100 ($\alpha = 0.001$)	CIFAR100 ($\alpha = 0.01$)
FedAdam [61]	33.52%	62.57%	30.85%	37.16%
FedDyn [1]	51.67%	81.03%	50.86%	53.79%
FedNova [71]	53.27%	84.26%	56.06%	58.47%
TCT	**83.02%**	**89.21%**	**69.07%**	**69.66%**

B.2 Results of Other Architectures

In Section 5, we use batch normalization [32] as the default normalization layer on CIFAR10 and CIFAR100 datasets, and we denote the ResNet-18 with batch normalization layers by ResNet-18-BN. In Table 4, we consider group normalization [79] on CIFAR10 and CIFAR100 and let ResNet-18-GN denote the ResNet-18 with group normalization. We set `num_groups=2` in group normalization layers. As shown in Table 4, TCT achieves better performance than FedAvg with ResNet-18-GN on both CIFAR10 and CIFAR100 datasets. Our experiments indicate that in extremely heterogeneous settings, group norm is insufficient to fix FedAvg.

Table 4: The top-1 test accuracy ($\%$) of our algorithm (TCT) vs. FedAvg(-GN) evaluated on CIFAR10 and CIFAR100. We vary the degree of data heterogeneity by controlling the α parameter of the symmetric Dirichlet distribution $\text{Dir}_K(\alpha)$ and the `#C` parameter for assigning how many labels each client owns. Higher accuracy is better. The highest top-1 accuracy in each setting is highlighted in **bold**.

Datasets	Architectures	Methods	Non-i.i.d. degree			
			`#C` $= 1$	`#C` $= 2$	$\alpha = 0.1$	$\alpha = 0.5$
CIFAR-10	ResNet-18-GN	FedAvg	21.23%	56.80%	84.72%	89.03%
	ResNet-18-BN	FedAvg	11.27%	56.86%	82.60%	90.43%
	ResNet-18-BN	*TCT*	**49.92%**	**83.02%**	**89.21%**	**91.10%**
			$\alpha = 0.001$	$\alpha = 0.01$	$\alpha = 0.1$	$\alpha = 0.5$
CIFAR-100	ResNet-18-GN	FedAvg	47.60%	48.60%	53.29%	55.39%
	ResNet-18-BN	FedAvg	53.89%	54.22%	63.49%	67.65%
	ResNet-18-BN	*TCT*	**68.42%**	**69.07%**	**69.66%**	**69.68%**

B.3 Additional Experimental Results of the Effect of Stage 1 Communication Round for TCT

In Figure 6, we provide additional results of the effect of T_1 for TCT on CIFAR10 and CIFAR100 datasets. We find that TCT outperforms existing algorithm across all T_1 communication rounds, where $T_1 \geq 20$. Extending the number of rounds for the baseline algorithms to 200 rounds does not improve their performance. In contrast, running 60 rounds of bootstrapping using FedAvg followed by 40 rounds of TCT gives near-optimal performance across all settings.

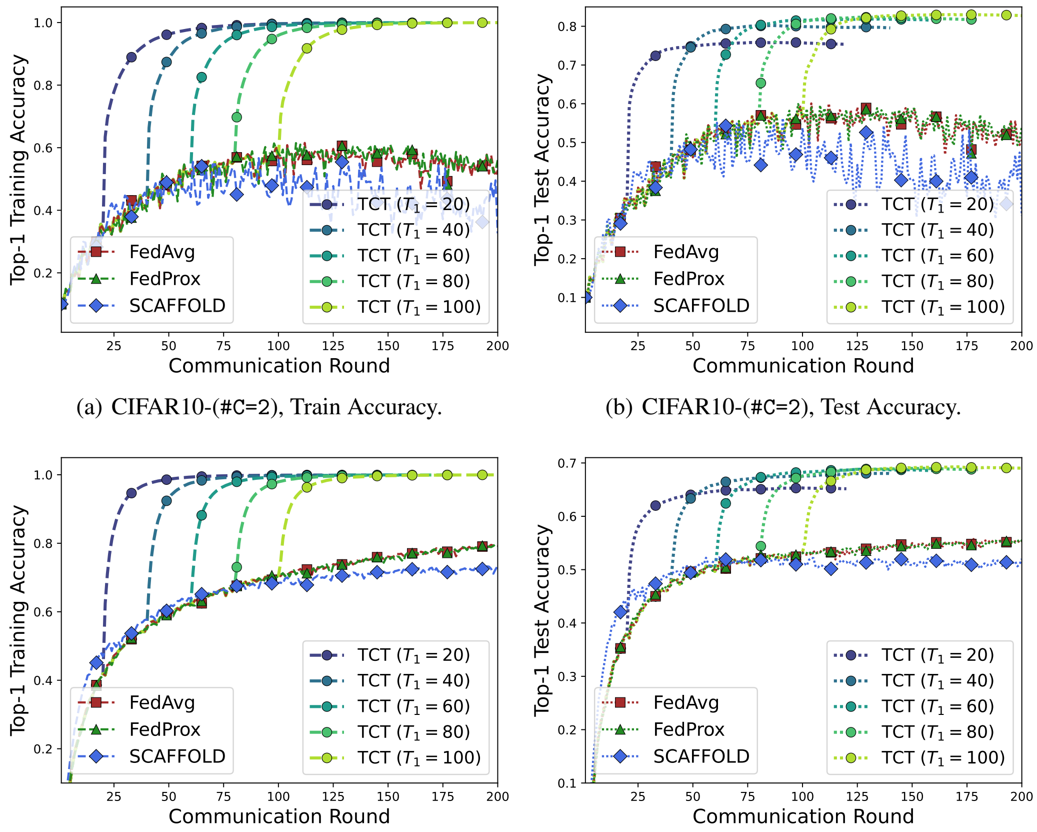

(a) CIFAR10-(#C=2), Train Accuracy. (b) CIFAR10-(#C=2), Test Accuracy.

(c) CIFAR100-($\alpha = 0.01$), Train Accuracy. (d) CIFAR100-($\alpha = 0.01$), Test Accuracy.

Figure 6: We evaluate TCT on using checkpoints saved at different communication rounds T_1 in **Stage 1**. We compare TCT to existing algorithm, including FedAvg, FedProx, and SCAFFOLD. For all three existing algorithms, we visualize the results of local learning rate $\eta = 0.1$. The train/test accuracy results in the first T_1 communication rounds of TCT are the same as FedAvg. For example, "TCT ($T_1 = 20$)" corresponds to training the model with FedAvg for $T_1 = 20$ rounds in **Stage 1** and then running 100 rounds of SCAFFOLD for solving the linear regression problem in **Stage 2**. Plots **(a)** and **(c)** display training accuracy and **(b)** and **(d)** display test accuracy.

B.4 Additional Experimental Results of Pre-trained Models

In Table 5 and Figure 7, we provide additional results of the effect of pre-training for FedAvg and TCT on CIFAR10 and CIFAR100 datasets. For both methods, we use the ResNet-18 pre-trained on ImageNet-1k [25] as the initialization. We use *FedAvg (last layer)* to denote applying FedAvg on learning the last linear layer of the model, i.e., layers except for the last linear layer are freezed during training. Compared to results in Table 2, we find that using pre-trained model as initialization largely improves the performance of both FedAvg and TCT. However, FedAvg still suffers from data heterogeneity. In contrast, TCT achieves similar performance as the centralized setting on both datasets across different degrees of data heterogeneity.

Table 5: The top-1 test accuracy $(\%)$ of our algorithm (TCT) vs. FedAvg evaluated on CIFAR10 and CIFAR100 with pre-trained model initialization. We vary the degree of data heterogeneity by controlling the α parameter of the symmetric Dirichlet distribution $\mathrm{Dir}_K(\alpha)$ and the `#C` parameter for assigning how many labels each client owns. Higher accuracy is better. The highest top-1 accuracy in each setting is highlighted in **bold**.

Methods	Datasets			
	CIFAR10 (`#C` $= 2$)	CIFAR10 ($\alpha = 0.1$)	CIFAR100 ($\alpha = 0.001$)	CIFAR100 ($\alpha = 0.01$)
Centralized	95.13%	95.13%	80.65%	80.65%
FedAvg (last layer)	63.60%	75.16%	50.40%	51.97%
FedAvg	64.73%	84.25%	62.23%	63.81%
TCT	**92.97%**	**93.70%**	**79.25%**	**79.55%**

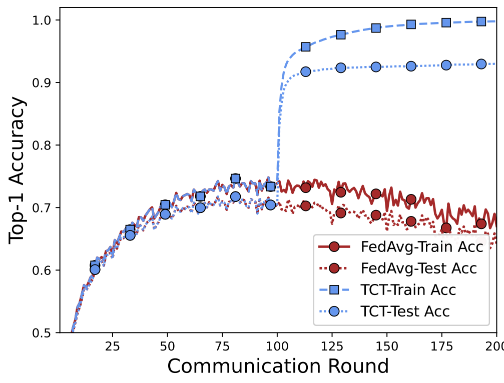

(a) CIFAR10-(`#C=2`).

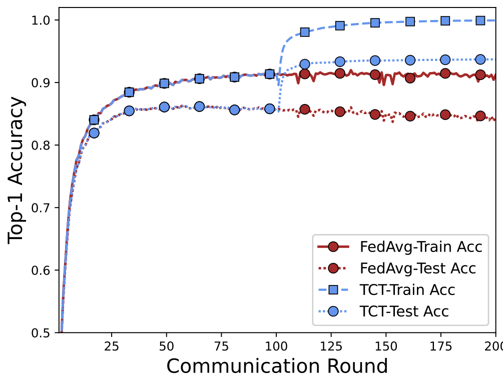

(b) CIFAR10-($\alpha = 0.1$).

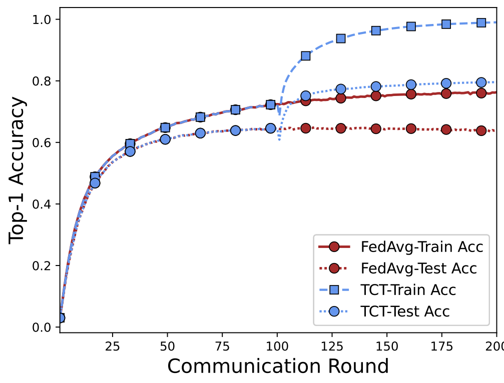

(c) CIFAR100-($\alpha = 0.01$).

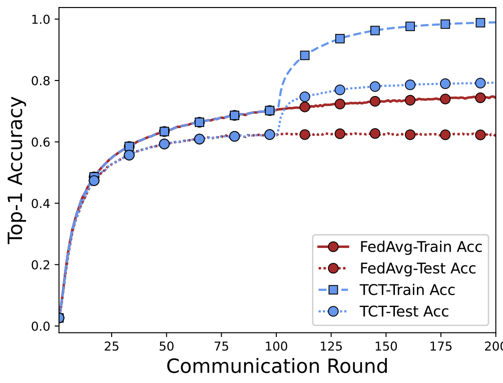

(d) CIFAR100-($\alpha = 0.001$).

Figure 7: We evaluate FedAvg and TCT on CIFAR10 and CIFAR100 datasets with pre-trained ResNet-18. Plots **(a)** and **(b)** display training/test accuracy on the CIFAR10 dataset and **(c)** and **(d)** display training/test accuracy on the CIFAR100 dataset.

B.5 Additional Experimental Results of One-round Communication

In Table 6, we provide additional results of TCT on CIFAR10 and CIFAR100 datasets with one communication round in TCT-Stage 2. Specifically, we set the number of local steps $M = 500$, local learning rate $\eta = 0.00005$, and the total number of communication round $T = 1$ in TCT-Stage 2. The results are summarized in Table 6. With only one communication round in TCT-Stage 2, TCT still achieves better performance than FedAvg in three out of four settings in Table 6. On the other hand, we recommend setting the communication round in TCT-Stage 2 larger than 10 for our method TCT in order to achieve satisfying performance.

Table 6: The top-1 test accuracy (%) of our algorithm (TCT) on CIFAR10 and CIFAR100 with one communication round in TCT-Stage 2.

Methods	**Datasets**			
	CIFAR10 (#C $= 2$)	CIFAR10 ($\alpha = 0.01$)	CIFAR100 ($\alpha = 0.001$)	CIFAR100 ($\alpha = 0.01$)
FedAvg	56.86%	82.60%	53.89%	54.22%
TCT	83.02%	89.21%	68.42%	69.07%
TCT-OneRound	64.94%	82.62%	55.50%	57.51%

B.6 Additional Experimental Results of Large Number of Clients

We study the performance of our proposed algorithm as well as existing algorithms in the large number of clients setting, where we consider the number of clients $K = 50$ on CIFAR100 with $\alpha = 0.001$. The results are summarized in Table 7. We find our proposed method (TCT: 45.32%) significantly outperforms existing methods (best test accuracy: 16.70%).

Table 7: The top-1 accuracy (%) of our algorithm (TCT) vs. state-of-the-art federated learning algorithms evaluated on CIFAR100 with a large number of clients. We set the degree of data heterogeneity parameter $\alpha = 0.001$ and set the total number of clients $K = 50$. Higher accuracy is better. The highest top-1 accuracy is highlighted in **bold**.

Dataset	**Architecture**	**# Clients**	**FedAvg**	**FedProx**	**SCAFFOLD**	**TCT**
CIFAR100 ($\alpha = 0.001$)	ResNet-18	50	16.70%	16.24%	13.41%	**45.32%**

B.7 Additional Ablations

Effect of local learning rate for TCT and FedAdam. As mentioned in Reddi et al. [61], FedAdam is more robust to the choice of local learning rate compared to FedAvg. We conduct additional ablations on the effect of local learning rate for TCT as well as FedAdam [61] on the CIFAR10 dataset. For each algorithm, we first select a base local learning rate η_{base} and then vary the local learning rate $\eta \in \{\eta_{\text{base}} \cdot 10^{0}, \eta_{\text{base}} \cdot 10^{-0.5}, \eta_{\text{base}} \cdot 10^{-1.0}, \eta_{\text{base}} \cdot 10^{-1.5}\}$. The results are summarized in Table 8. Compared to FedAdam, we find that TCT is much less sensitive to the choice of local learning rate.

Table 8: The top-1 test accuracy (%) of our algorithm (TCT) and FedAdam [61] evaluated on the CIFAR10 dataset. We vary the local learning rate for both algorithms. Higher accuracy is better.

Datasets	**Methods**	**Local learning rate**			
	($\eta_{\text{base}} = 10^{-4}$)	$\eta = \eta_{\text{base}} \cdot 10^{0}$	$\eta = \eta_{\text{base}} \cdot 10^{-0.5}$	$\eta = \eta_{\text{base}} \cdot 10^{-1.0}$	$\eta = \eta_{\text{base}} \cdot 10^{-1.5}$
CIFAR10-(#C=2)	TCT	82.12%	83.60%	83.51%	82.37%
CIFAR10-($\alpha = 0.1$)	TCT	88.68%	89.27%	89.23%	89.15%
	($\eta_{\text{base}} = 10^{-1.5}$)	$\eta = \eta_{\text{base}} \cdot 10^{0}$	$\eta = \eta_{\text{base}} \cdot 10^{-0.5}$	$\eta = \eta_{\text{base}} \cdot 10^{-1.0}$	$\eta = \eta_{\text{base}} \cdot 10^{-1.5}$
CIFAR10-(#C=2)	FedAdam [61]	31.29%	33.52%	26.20%	14.96%
CIFAR10-($\alpha = 0.1$)	FedAdam [61]	10.31%	37.26%	62.57%	49.18%

Effect of local learning rate and number of local steps for TCT. We conduct additional ablations on the effect of both the local learning rate η and the number of local steps M for TCT on CIFAR10 and CIFAR100 datasets. The results in Table 9 and Table 10 indicate that TCT is robust to the choice of the local learning rate η and the number of local steps M. We find that as the number of steps increases, the learning rate should predictably decrease. The performance is relatively stable along the diagonal, indicating that it is the product $M \cdot \eta$ which affects accuracy.

Table 9: The top-1 test accuracy ($\%$) of our algorithm (TCT) evaluated on the CIFAR10 dataset. We consider CIFAR10-(`#C=2`) and we set $\eta_{\text{base}} = 10^{-4}$. We vary both the local learning rate and the number of local steps for TCT. Higher accuracy is better.

Number of local steps	Local learning rate			
	$\eta = \eta_{\text{base}} \cdot 10^{0}$	$\eta = \eta_{\text{base}} \cdot 10^{-0.5}$	$\eta = \eta_{\text{base}} \cdot 10^{-1.0}$	$\eta = \eta_{\text{base}} \cdot 10^{-1.5}$
$M = 50$	83.51%	82.37%	80.67%	78.14%
$M = 100$	83.59%	83.35%	81.73%	79.71%
$M = 500$	82.12%	83.60%	83.51%	82.37%
$M = 1000$	80.78%	82.92%	83.59%	83.35%

Table 10: The top-1 test accuracy ($\%$) of our algorithm (TCT) evaluated on the CIFAR100 dataset. We consider CIFAR100-($\alpha = 0.01$) and we set $\eta_{\text{base}} = 10^{-4}$. We vary both the local learning rate and the number of local steps for TCT. Higher accuracy is better.

Number of local steps	Local learning rate			
	$\eta = \eta_{\text{base}} \cdot 10^{0}$	$\eta = \eta_{\text{base}} \cdot 10^{-0.5}$	$\eta = \eta_{\text{base}} \cdot 10^{-1.0}$	$\eta = \eta_{\text{base}} \cdot 10^{-1.5}$
$M = 50$	69.12%	67.31%	64.61%	61.34%
$M = 100$	69.54%	68.48%	66.43%	63.42%
$M = 500$	69.03%	69.60%	69.12%	67.31%
$M = 1000$	68.38%	69.42%	69.54%	68.48%

Effect of training loss for TCT-Stage 2. We compare the performance of quadratic loss (defined in Eq. (1)) and cross-entropy loss (i.e., applying the cross-entropy loss for learning the linear model in TCT-Stage 2, denoted by *TCT-CE*) for TCT in Table 11. As shown in Table 11, we find quadratic loss indeed achieves better performance than cross-entropy loss for TCT.

Effect of subsampling for TCT-Stage 2. We study the performance of full eNTK representation in TCT-Stage 2 (i.e., without random subsampling) to investigate the role of the subsampling approximation. We provide the results in Table 11. As shown in Table 11, applying full eNTK representations slightly improves (improvements are smaller than 2% across all settings) the performance of TCT on CIFAR10/100. On the other hand, using subsampled eNTK reduces the communication cost more than 100x compared to the full eNTK and existing federated learning algorithms (#parameter of the whole model: 11,169,345, #parameters of the subsample eNTK: 100,000).

Applying last layer representations in TCT-Stage 2. We study the performance of only applying last layer representations in TCT-Stage 2, and the results are summarized in Table 12. From Table 12, we find that applying eNTK representations with high dimension (i.e., $p = 100,000$) outperforms using the representations before the last layer only, especially in the settings with high degrees of data heterogeneity. These results provide further evidence on applying eNTK features instead of the representations before the last layer features.

Table 11: The top-1 accuracy (%) of our algorithm (TCT) vs. TCT-CE, TCT-full-eNTK on FMNIST, CIFAR10, and CIFAR100. We vary the degree of data heterogeneity by controlling the α parameter of the symmetric Dirichlet distribution $\mathrm{Dir}_K(\alpha)$ and the `#C` parameter for assigning how many labels each client owns. Higher accuracy is better. TCT-CE represents the variant of TCT where we apply cross-entropy loss in Stage 2 of TCT. TCT-full-eNTK represents the variant of TCT where we use the full eNTK representation (without subsampling) in Stage 1 of TCT.

Datasets	**Architectures**	**Methods**	**Non-i.i.d. degree**			
			`#C` $= 1$	`#C` $= 2$	$\alpha = 0.1$	$\alpha = 0.5$
FMNIST	SimpleCNN	*TCT*	86.32%	90.33%	90.78%	91.13%
		TCT-CE	86.50%	89.23%	89.66%	90.15%
		TCT-full-eNTK	86.32%	90.36%	90.90%	91.18%
			`#C` $= 1$	`#C` $= 2$	$\alpha = 0.1$	$\alpha = 0.5$
CIFAR-10	ResNet-18	*TCT*	49.92%	83.02%	89.21%	91.10%
		TCT-CE	45.13%	81.06%	88.03%	91.12%
		TCT-full-eNTK	50.38%	84.92%	89.72%	91.69%
			$\alpha = 0.001$	$\alpha = 0.01$	$\alpha = 0.1$	$\alpha = 0.5$
CIFAR-100	ResNet-18	*TCT*	68.42%	69.07%	69.66%	69.68%
		TCT-CE	63.46%	64.08%	65.22%	66.07%
		TCT-full-eNTK	69.81%	70.05%	70.12%	70.91%

Table 12: The top-1 accuracy (%) of our algorithm (TCT) vs. TCT-last-layer on FMNIST, CIFAR10, and CIFAR100. We vary the degree of data heterogeneity by controlling the α parameter of the symmetric Dirichlet distribution $\mathrm{Dir}_K(\alpha)$ and the `#C` parameter for assigning how many labels each client owns. Higher accuracy is better. The highest top-1 accuracy in each setting is highlighted in **bold**. TCT-last-layer represents the variant of TCT where we apply the representations of last layer and cross-entropy loss in Stage 2 of TCT.

Datasets	**Architectures**	**Methods**	**Non-i.i.d. degree**			
			`#C` $= 1$	`#C` $= 2$	$\alpha = 0.1$	$\alpha = 0.5$
FMNIST	SimpleCNN	*TCT*	**86.32%**	**90.33%**	**90.78%**	**91.13%**
		TCT-last-layer	60.43%	83.96%	86.01%	89.33%
			`#C` $= 1$	`#C` $= 2$	$\alpha = 0.1$	$\alpha = 0.5$
CIFAR-10	ResNet-18	*TCT*	**49.92%**	**83.02%**	**89.21%**	**91.10%**
		TCT-last-layer	35.51%	74.55%	86.57%	90.76%
			$\alpha = 0.001$	$\alpha = 0.01$	$\alpha = 0.1$	$\alpha = 0.5$
CIFAR-100	ResNet-18	*TCT*	**68.42%**	**69.07%**	**69.66%**	**69.68%**
		TCT-last-layer	59.80%	60.04%	64.98%	66.22%